# A Proposed Stereo Matching Algorithm for Noisy Sets of Color Images

Lior Shamir *

*Image Informatics and Computational Biology Unit, Laboratory of Genetics, NIA, NIH*
*333 Cassell Dr., Suite 3000, Baltimore, MD 21224*

**Abstract**

Modeling the world in three dimensions has been attracting a growing interest both in applications and science. In many cases, such 3D models are achieved by triangulating corresponding features recorded by several images of the same field taken from different points of view. This, however, requires the ability to match corresponding image elements detected in different images.

In this paper, an algorithm for stereo matching in noisy pairs of outdoor images is described. The proposed algorithm applies a standard window based correlation, but uses a fuzzy logic-based similarity function that models the HSV color space. This fuzzy logic modeling allows a robust color comparison that can tolerate a certain degree of changes in the illumination conditions, and can be used for finding corresponding pixels in noisy sets of images. While the proposed algorithm does not introduce an improvement over existing methods in ideal conditions, experiments suggest that it provides significantly better results when the images in the set are relatively different from each other, and can be effective for matching corresponding features in images taken in different weather conditions, different position of the sun, different optics, or other real-life situation in which pinhole conditions are not available.

*Key words:* Stereo Matching, Stereo Vision, Fuzzy Logic

## 1 Introduction

Binocular vision is commonly used for constructing 3D models by using two (or more) images of the same field taken from two cameras. The horizontal

* Corresponding author: Tel: (410) 558-8682 Fax: (410) 558-8331
*Email address:* shamirl@mail.nih.gov (Lior Shamir).

disparity of scene elements captured in the two images can be measured, and the depth of image features can be deduced. This approach is commonly used in GIS and remote sensing applications for the purpose of 3D modeling of urban areas (Karner, 2004; Baillard & Dissard, 2000), individual trees (Larsen & Rudemo, 2004), surface reconstruction (Bolle & Vemuri, 1991; Cochran & Medioni, 1992; Copper et al., 2005; Fua, 1993; Fua & Leclerc, 1995; Lin & Tomasi, 2004; Takizawa & Yamamoto, 2006) or general surface points of interest (Zhou et al., 1996; Pong et al., 1989).

While the triangulation of corresponding elements detected in two (or more) images is fairly simple, the more challenging problem in this process is finding corresponding features in the images. The problem of associating features in stereo images of the same field is sometimes referred to as *the stereo correspondence problem.*

In the last two decades, the correspondence problem has attracted a considerable amount of attention, and several algorithms have been proposed and implemented (Bolles et al., 1987; Kolmogorov et al., 2001; Ohta & Kanade, 1985; Scharstein & Szeliski, 1998, 2002). Approaches to the stereo correspondence problem can be divided into two major categories: feature based and pixel based. In feature based correspondence, low-level features such as edges and corners are detected and used for finding correspondences, and the remaining non-featured pixels are determined by interpolation of the detected matching features. Pixel based methods use the distribution of pixel intensities for finding corresponding pixels. Generally, pixel based methods have gained more popularity over the years. However, while this approach can provide good results in high quality images taken under ideal conditions, its effectiveness is limited when the two images are taken under different illumination condition such as different position of the sun, presence\absence of other sources of light, inaccurate optics, different weather conditions, etc'. In fact, stereo data sets such as (Scharstein & Szeliski, 2002) and (Scharstein & Szeliski, 2003), which are designed specifically for testing stereo matching algorithms do not include noisy pairs of outdoor images, and little has yet been reported on solving the correspondence problem under such conditions. Approaches to the stereo correspondence problem that can handle a certain degree of noise in the images include non-parametric Rank and Census transforms (Zabin & Woodfill, 1994; Banks & Bennamoun, 2001) and energy minimization using maximization of mutual information (Kim, Kolmogorov & Zabih, 2003). Although the performance of these algorithms is not dependent on the absolute values of the pixel intensities, they assume a certain level of consistency within the local neighborhoods of the corresponding pixels. However, in cases of extremely noisy sets of stereo images the relative order of intensities within the local neighborhoods might not always be consistent.

In this paper we describe a stereo correspondence algorithm designed for noisy

sets of images that addresses the problem by using a robust pixel similarity function. Noisy sets, for this matter, are sets of images in which the left image and the right image were taken under different illumination condition, different weather, or by different instruments. The core of the algorithm is a fuzzy logic-based similarity function that provides a comparison of colors, rather than comparing the pixel intensities. This comparison can tolerate differences in the illumination conditions, so that pixels with the same color can be associated even if their intensities in the images are different. This feature allows the algorithm to match corresponding pixels in pairs of images that are slightly different from each other in terms of weather conditions, luminosity, optics etc.

In Section 2 the fuzzy logic-based color similarity function is described, in Section 3 the upper level algorithm for finding corresponding pixel is discussed, and in Section 4 experimental results are presented.

## 2 Fuzzy Logic-based Color Similarity Function

Fuzzy Logic is commonly used as an interface between logic and human perception (Zadeh, 1974, 1988). The similarity function is based on a fuzzy logic model that aims to follow a human perception of color differences. This can be achieved by using fuzzy logic modeling of the HSV color space, which is more intuitive than other proposed color spaces such as RGB (Smith, 1978). Since in the HSV color space each color is defined by three values (H, S, V), the fuzzy logic model has three antecedent variables $\Delta_H$, $\Delta_S$ and $\Delta_V$, which are the differences in the H, S and V components of the two pixels. The domain of these variables is the interval (0,240). The consequent variable is the normalized difference between the two pixels, and its domain is the interval (0,1).

### *2.1 Fuzzy Sets*

The fuzzy logic model uses 4 fuzzy sets for $\Delta_H$, 4 fuzzy sets for $\Delta_S$ and 4 fuzzy sets for $\Delta_V$. All membership functions are in the form of *triangular* and *trapezoidal* functions (Zadeh, 1965), which are efficient in terms of computational complexity (Johanyak & Kovacs, 2006). Since the similarity function should be called very many times when processing a set of two stereo images, the low computational complexity of the fuzzification is an important concern.

The fuzzy sets of the antecedent variable $\Delta_H$ are *h_tiny*, *h_small*, *h_medium* and *h_large*, and their membership functions are described in Figure 1.

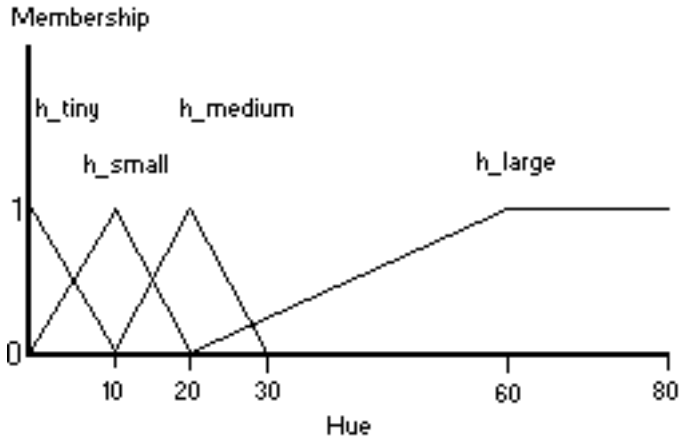


Fig. 1. The membership functions defined on $\Delta_H$

$\Delta_S$ is defined using the fuzzy sets *s_tiny*, *s_small*, *s_medium* and *s_large* as described in Figure 2.

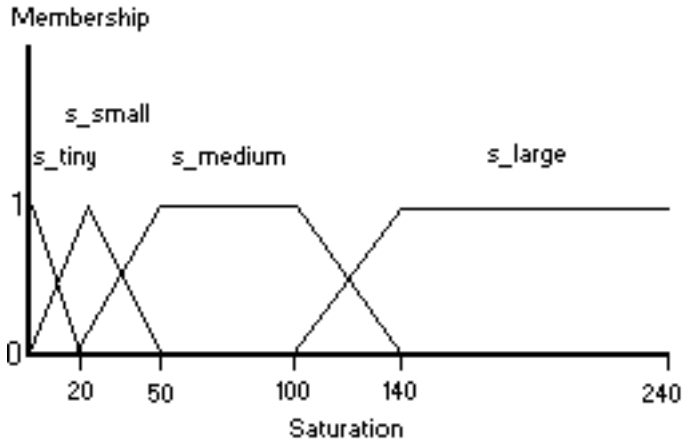


Fig. 2. The membership functions defined on $\Delta_S$

$\Delta_V$ is defined using the fuzzy sets *v_tiny*, *v_small*, *v_medium* and *v_large* as described in Figure 3.

The defuzzification method used in this model is *weighted average* (Takagi & Sugeno, 1983, 1985), for its low computational complexity (Regattieri Delgado et al., 2000). Since *weighted average* is used, fuzzy sets should not be defined for the consequent fuzzy variable.

The values of the points of maximum of the membership functions and their intersection with the X-axis are determined empirically by observing the values of HSV triples of different colors, and are based on the human intuition of the perception of color (Shamir, 2006). Typically, the density of the fuzzy sets is higher in the range of the lower values (smaller difference) than in the range of the higher values (greater difference). This is because a large difference in any of the values (H, S or V) is an indication of color difference, regardless the

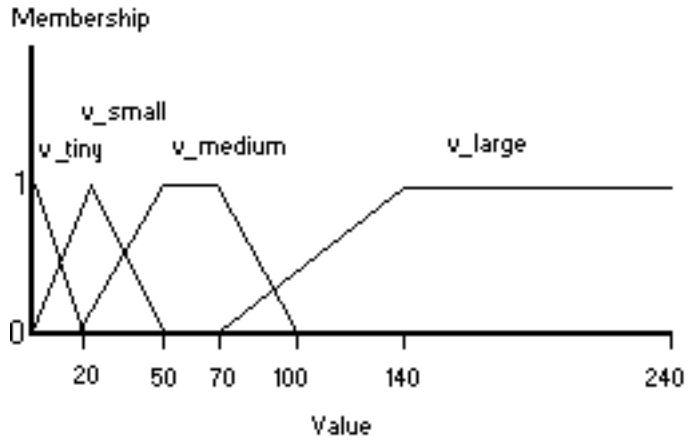


Fig. 3. The membership functions defined on $\Delta_V$

values of the other components. For instance, comparing the two HSV triples (20,15,240) and (20,12,100) leads to the conclusion that the colors represented by the two HSV triples are different. This is due to the large difference in the values of the $V$ component. If the above two triples are different, it can be deduced that any value of the $V$ component in the second HSV triple, such that the difference between the two $V$ values is greater than 140, will provide a different color than the first triple (20,15,240). Therefore, there will be no effective use of more fuzzy sets defined on $\Delta_V$ in the interval (140,240). In the lower values, however, the effect of the dependencies between the different dimensions of the color space is significant, and therefore a higher density of fuzzy sets leads to higher accuracy.

The number of fuzzy sets can be modified according to the specific needs of the model. More membership functions will typically provide better accuracy, but with the sacrifice of computational complexity. However, experiments suggest that increasing the number of membership functions does not noticeably increase the accuracy presented in Section 4.

### *2.2 Fuzzy Rules*

The purpose of the fuzzy rules is to define the estimated difference of two colors based on the differences of their H, S and V components. The rules can be defined by a set of natural language rules such as rules 1 and 2 below:
1. If the difference of the hue is small, the difference of the saturation is small and the difference of the value is small, then the two pixels share the same color.
2. If the difference of the hue is medium, the difference of the saturation is medium and the difference of the value is large, then the two pixels do not share the same color.

In order to obtain a model that follows the perception described above, the natural language rules are compiled into fuzzy rules using the fuzzy sets described in Figures 1, 2 and 3. For standard RGB images, this set of fuzzy rules can be used without the requirement of a last step of fine-tuning, so that no efforts should be sacrificed for data collection or tuning.

Since this model has 4 fuzzy sets for $\Delta_H$, 4 fuzzy sets for $\Delta_S$ and 4 fuzzy sets for $\Delta_V$, the total number of fuzzy rules is $4\times4\times4=64$. Since the *weighted average* defuzzification (Takagi & Sugeno, 1983, 1985) is used, the consequent parts of the rules are crisp values rather than fuzzy sets. The domain of these values is {0,1}, such that 1 means that the colors of the two pixels are different and 0 means that the two pixels share the same color. The fuzzy rules used in this model are listed below:

h_tiny, s_tiny, v_tiny $\longmapsto$ 0
h_tiny, s_tiny, v_medium $\longmapsto$ 0
h_tiny, s_small, v_tiny $\longmapsto$ 0
h_tiny, s_small, v_medium $\longmapsto$ 0
h_tiny, s_medium, v_tiny $\longmapsto$ 0
h_tiny, s_medium, v_medium $\longmapsto$ 1
h_tiny, s_large, v_tiny $\longmapsto$ 1
h_tiny, s_large, v_medium $\longmapsto$ 1
h_small, s_tiny, v_tiny $\longmapsto$ 0
h_small, s_tiny, v_medium $\longmapsto$ 0
h_small, s_small, v_tiny $\longmapsto$ 0
h_small, s_small, v_medium $\longmapsto$ 0
h_small, s_medium, v_tiny $\longmapsto$ 0
h_small, s_medium, v_medium $\longmapsto$ 1
h_small, s_large, v_tiny $\longmapsto$ 1
h_small, s_large, v_medium $\longmapsto$ 1
h_medium, s_tiny, v_tiny $\longmapsto$ 0
h_medium, s_tiny, v_medium $\longmapsto$ 0
h_medium, s_small, v_tiny $\longmapsto$ 0
h_medium, s_small, v_medium $\longmapsto$ 1
h_medium, s_medium, v_tiny $\longmapsto$ 0
h_medium, s_medium, v_medium $\longmapsto$ 1
h_medium, s_large, v_tiny $\longmapsto$ 1
h_medium, s_large, v_medium $\longmapsto$ 1
h_large, s_tiny, v_tiny $\longmapsto$ 1
h_large, s_tiny, v_medium $\longmapsto$ 1
h_large, s_small, v_tiny $\longmapsto$ 1
h_large, s_small, v_medium $\longmapsto$ 1
h_large, s_medium, v_tiny $\longmapsto$ 1
h_large, s_medium, v_medium $\longmapsto$ 1
h_large, s_large, v_tiny $\longmapsto$ 1
h_large, s_large, v_medium $\longmapsto$ 1

h_tiny, s_tiny, v_small $\longmapsto$ 0
h_tiny, s_tiny, v_large $\longmapsto$ 1
h_tiny, s_small, v_small $\longmapsto$ 0
h_tiny, s_small, v_large $\longmapsto$ 1
h_tiny, s_medium, v_small $\longmapsto$ 0
h_tiny, s_medium, v_large $\longmapsto$ 1
h_tiny, s_large, v_small $\longmapsto$ 1
h_tiny, s_large, v_large $\longmapsto$ 1
h_small, s_tiny, v_small $\longmapsto$ 0
h_small, s_tiny, v_large $\longmapsto$ 1
h_small, s_small, v_small $\longmapsto$ 0
h_small, s_small, v_large $\longmapsto$ 1
h_small, s_medium, v_small $\longmapsto$ 0
h_small, s_medium, v_large $\longmapsto$ 1
h_small, s_large, v_small $\longmapsto$ 1
h_small, s_large, v_large $\longmapsto$ 1
h_medium, s_tiny, v_small $\longmapsto$ 0
h_medium, s_tiny, v_large $\longmapsto$ 1
h_medium, s_small, v_small $\longmapsto$ 0
h_medium, s_small, v_large $\longmapsto$ 1
h_medium, s_medium, v_small $\longmapsto$ 1
h_medium, s_medium, v_large $\longmapsto$ 1
h_medium, s_large, v_small $\longmapsto$ 1
h_medium, s_large, v_large $\longmapsto$ 1
h_large, s_tiny, v_small $\longmapsto$ 1
h_large, s_tiny, v_large $\longmapsto$ 1
h_large, s_small, v_small $\longmapsto$ 1
h_large, s_small, v_large $\longmapsto$ 1
h_large, s_medium, v_small $\longmapsto$ 1
h_large, s_medium, v_large $\longmapsto$ 1
h_large, s_large, v_small $\longmapsto$ 1
h_large, s_large, v_large $\longmapsto$ 1

## 3 Finding Corresponding Pixels

The advantage of the fuzzy logic-based similarity function is that the pixel comparison is not performed by simply using the difference between the intensities of the two pixels, but by applying a human perception-based model of color comparison that can tolerate a certain degree of noise.

The corresponding pixels are found by using a standard window-based correlation (Forstner & Pertl, 1986; Hannah, 1989; Matthies et al., 1989; Wood, 1983) using the similarity function described in Section 2. By using the epipolar constraint, the window is shifted along the epipolar line of the other image, so that the search space is reduced to just one line (Ohta & Kanade, 1985). The sum of differences is given in Equation 1.

$$SD = \Sigma_{i=u-h,j=v-h}^{i=u+h,j=v+h} f(L_{x+i,y+j}, R_{u+i,v+j}) \quad (1)$$

Where $L$ is the left image, $R$ is the right image, $(x, y)$ and $(u, v)$ are the image coordinates of compared pixels, $h$ is the half width size of the window and $f$ is the fuzzy logic based similarity function described in Section 2.

As indicated by (Kanade & Okutomi, 1994), a fixed window size is not an optimal policy since the window must be large enough to include enough intensity variation for reliable matching, but small enough to avoid the effects of projective distortion. Therefore, if a good match is not found using a small window, the width size of the window is doubled and another search is initiated. This continues until a good match is found, or the window is larger than half the image.

A good match, for this matter, is defined by the proposed algorithm as a match that its sum of differences is significantly lower than all other possible matches. If the sum of differences of the second-best match is greater by at least 20%, then a match is assumed. Otherwise, any match that its sum of differences is smaller than 120% of the minimum sum of differences is examined with a window size that is four times the size of the one used in the previous search. This continues until a match is found, or until the window is larger than half the image, in which case the best match in the last search is taken. This policy uses a larger window only if a small window does not provide a sufficient signal (color difference) to noise ratio.

Neighboring pixels might provide very close sums of differences. Therefore, in cases where a second pass with a larger window is needed, only the pixel that provides the best match (comparing to its neighbors) is checked, without checking its neighbors. For this matter, two neighboring pixels are defined as two pixels on the same scan-line that the distance between them is smaller

Fig. 4. Left image of Hancock, Michigan

than the half width size of the window. This policy significantly reduces the number of pixels that should be checked with a larger window, which is a computationally demanding task.

## 4 Experimental Results

Figures 4 and 5 are two images of Hancock, Michigan, taken from two different locations 50 meters away from each other. Since each image was taken at a different time of the day, even an eyeball examination of the two images can easily lead to the conclusion that the two images are different from each other, introducing an extremely noisy set.

The performance of the proposed algorithm was tested by selecting 20 points of interest detected by applying a simple Kitchen-Rosenfeld corner detection algorithm (Kitchen & Rosenfeld, 1982). These points are shown in Figure 6.

Table 1 shows the number of points that their corresponding pixels were accurately detected in the right image. As can be seen from the table, the proposed algorithm found the matching pixels for all points of interest except one (the leftmost point in Figure 6), while other algorithms experienced difficulties in processing these noisy test data.

Figure 7 shows a comparison of the disparity maps (Bolles et al., 1987; Okutomi & Kanade, 1993; Scharstein & Szeliski, 2002) of Figure 4 using SSD,

Fig. 5. Right image of Hancock, Michigan

Fig. 6. Points of interest

Bayesian Diffusion (Scharstein & Szeliski, 1998), Graph Cuts (Kolmogorov et al., 2001), Non-parametric Local Transform (Rank and Census) (Zabin & Woodfill, 1994), and the proposed algorithm. In the presented pairs of images, pixels with computed disparity greater than the maximal disparity in the two images are considered as pixels with no disparity. Pixels for which no disparity was found are colored in black (Scharstein & Szeliski, 2003).

| Algorithm | Corresponding Pixels Detected |
|---|---|
| SDD | 0 |
| Graph Cuts | 7 |
| Bayesian Diffusion | 2 |
| Rank Transform | 10 |
| Census Transform | 7 |
| Proposed Algorithm | 19 |

Table 1
Number of corresponding pixels correctly detected for the points of interest of Figure 6

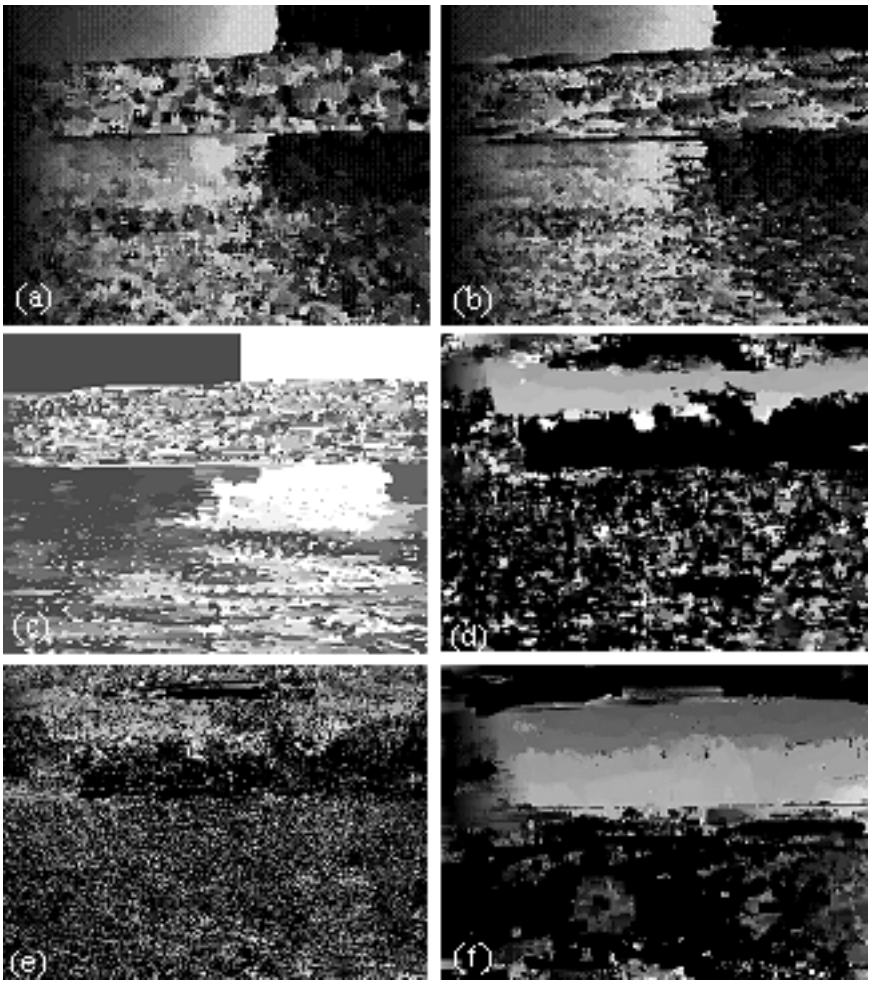


Fig. 7. Disparity maps computed using (a) SSD, (b) Bayesian Diffusion, (c) Graph Cuts, (d) Rank transform, (e) Census transform, and (f) the proposed algorithm.

As the disparity maps show, some existing stereo matching algorithms are not designed for extremely noisy sets of images such as the tested set, and provided poor performance that cannot be used for practical purposes. Rank Transform provided a better performance than the other tested algorithms, but due to the noisy nature of the stereo pairs, relative intensity within the local neighborhoods was not always consistent. The proposed algorithm per-


Fig. 8. Left (a) and right (b) images.

formed better than previously proposed algorithms in areas of the image which are rich with details, but failed to find matching pixels in flatter areas such as sky or water.

Figure 8 shows two (left and right) images taken by two different digital cameras. By adjusting the right image to the scale of the left image, the two images are of the same size. However, it is noticeable that the colors and luminosities of the two images are somewhat different. Figure 9 shows the disparity maps generated by using SSD, Bayesian Diffusion, Graph Cuts, Rank Transform, Census Transform, and the proposed algorithm.

While the proposed algorithm provides better accuracy in noisy outdoor images with large homogeneous regions, its performance is not comparable to previously proposed algorithms in image sets with many depth discontinuities. This is due to the policy of using increasingly larger windows until a corresponding pixel is found. Therefore, the proposed algorithm might not provide an optimal solution in cases where surface discontinuities are many. This can be demonstrated by Figure 11, showing the disparity map of Figure 10 (*venus*).

Figure 12 shows an attempt of using the algorithms with a first step of linear transformation of the intensities so that the sum of intensities in the left image is equal to the sum of intensities in the right image. This was done using the *convert* and *compare* utilities of ImageMagick (http://www.ImageMagick.org). The experiment shows that the transformation of the intensities did not contribute to the accuracy of the algorithms, which indicates that the absolute difference in the luminosity is not the main reason for the inaccuracy of the stereo matching algorithms, and that the images are different not only by their luminosity, but also by other effects due to the change in the position of the

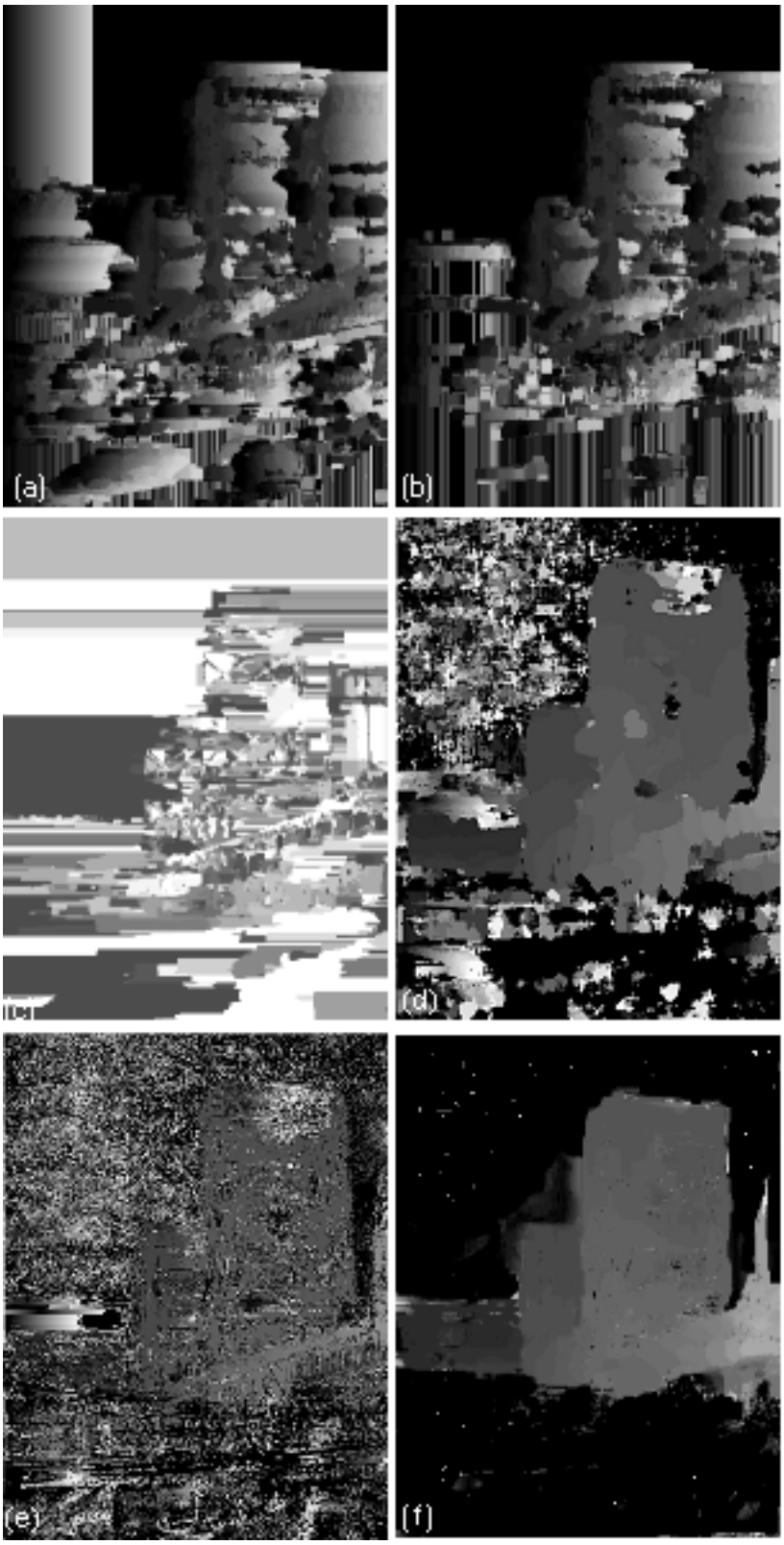


Fig. 9. Disparity maps computed using (a) SSD, (b) Bayesian Diffusion, (c) Graph Cuts, (d) Rank transform, (e) Census transform, and (f) the proposed algorithm.

Fig. 10. Left (a) and right (b) images.

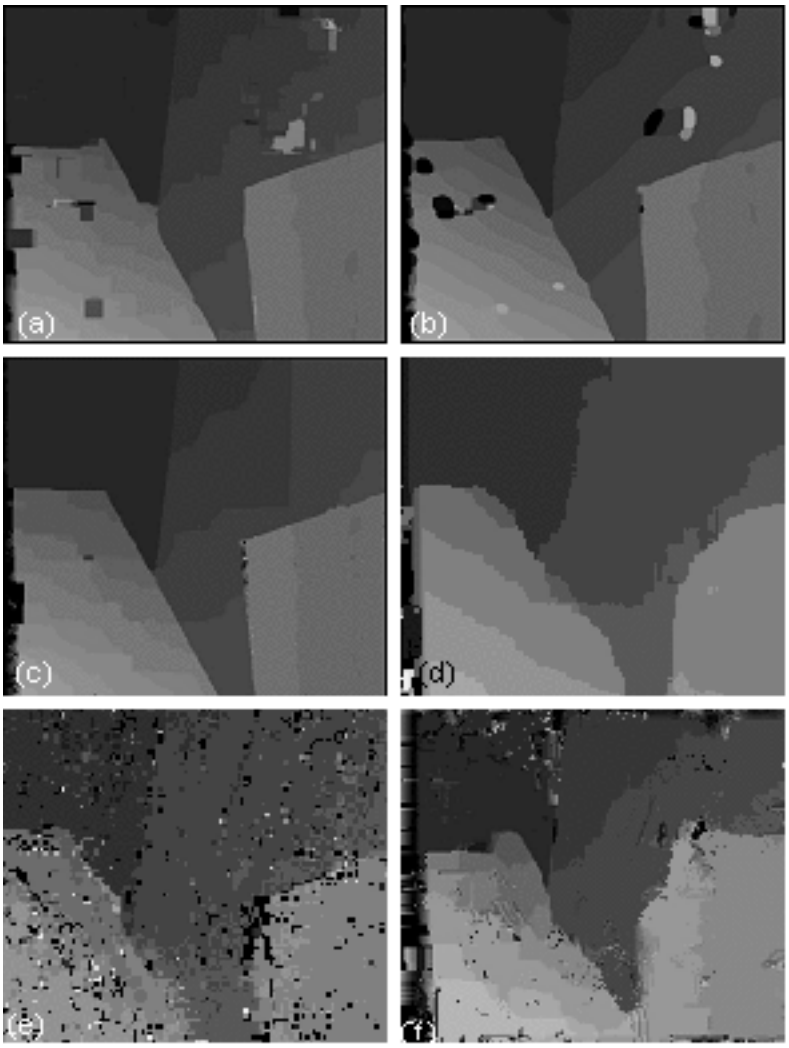


Fig. 11. Disparity maps computed using (a) SSD, (b) Bayesian Diffusion, (c) Graph Cuts, (d) Rank transform, (e) Census transform, and (f) the proposed algorithm.

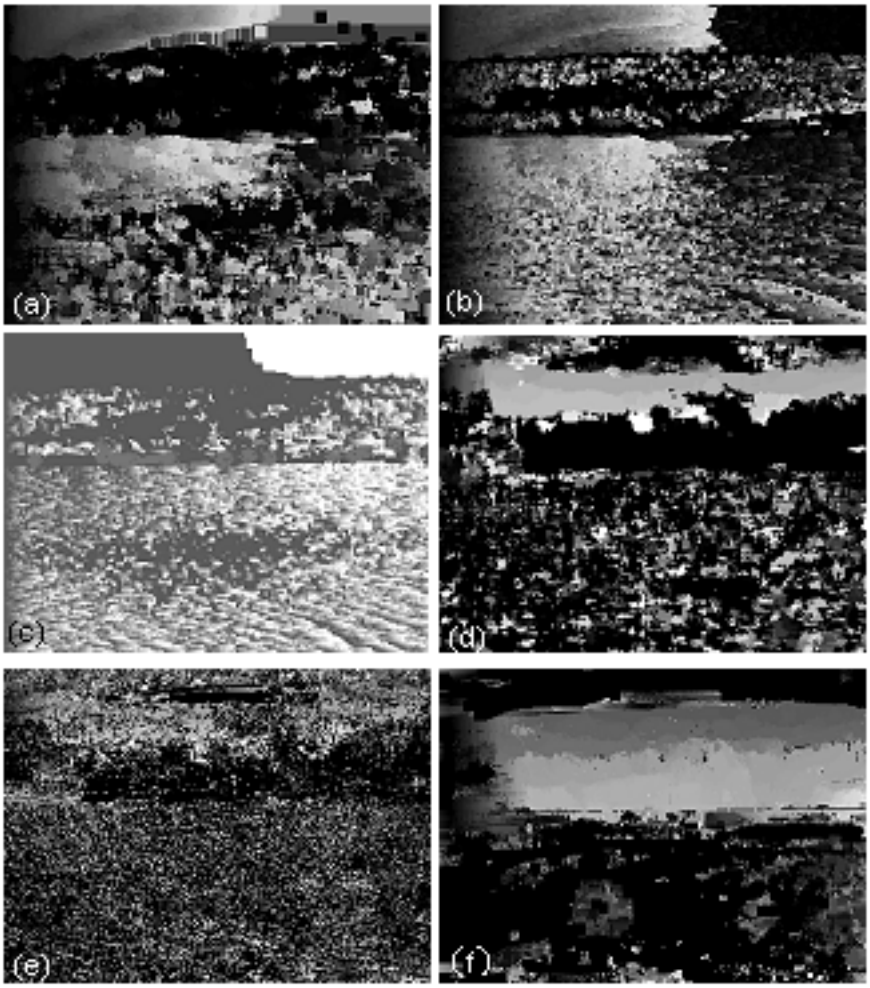


Fig. 12. Disparity maps computed using (a) SSD, (b) Bayesian Diffusion, (c) Graph Cuts, (d) Rank transform, (e) Census transform, and (f) the proposed algorithm.

sun and the different sensitivities of the different cameras, which cannot be easily characterized.

The experiments discussed in this section were all processed by the algorithm using the same set of fuzzy sets and fuzzy rules described in Section 2, so that no modifications or fine–tuning were needed. The downside of the proposed algorithm is its computational complexity. A system with an Intel Pentium 4 at 3.0 GHZ and 512 MB of RAM finds one pair of corresponding pixels in the $320 \times 240$ images of Figures 4 and 5 in $\sim$2 seconds. Therefore, generating a disparity map for a $320 \times 240$ image might take $\sim$42 hours. Although simple triangular membership functions are used, the pixel similarity function is still the bottleneck of the algorithm in terms of computational complexity. Since the similarity function is called for every pixel in the window, this relatively expensive comparison is the main source of the limited speed of the algorithm.

## 5 Conclusions

By using a fuzzy logic similarity function, corresponding pixels in noisy sets of stereo images can be found. This approach can be effective in situations of different weather conditions, different position of the sun, inaccurate optics, or other real-life situation in which pinhole conditions are not available. An example implementation of the proposed algorithm is available at http://www.phy.mtu.edu/~lshamir/downloads/correspondence/. The application runs under MS-Windows, and requires two input images (left and right). The application finds a corresponding pixel in the right image for each user-selected pixel in the left image, and can also compute the approximate distance by applying a simple triangulation based on a user-defined X parallax and the camera field of view. The distance is computed by assuming that the optical center is the center of the image and that the angle is linearly correlated with the distance (in pixels) from the image center. This straightforward model is often untrue, but since this problem is outside the scope of the paper the simple pinhole model is assumed, and used to give a rough estimation of the performance of the algorithm.

## References


Baillard, C., Dissard, O., 2000. A stereo matching algorithm for urban digital elevation models. Photogrammetric Engineering & Remote Sensing 66, 1119–1128.

Banks, J., Bennamoun, M., 2001. Reliability analysis of the rank transform for stereo matching. IEEE Transactions on Systems, Man and Cybernetics 31, 870–880.

Bolles, R.C., Baker, H.H., Marimont. D.H., 1987. Epipolarplane image analysis: An approach to determining structure from motion. International Journal of Computer Vision 1, 7–55.

Bolle R.M., Vemuri, B.C., 1991. On three-dimensional surface reconstruction methods. IEEE Transactions on Pattern Analysis and Machine Intelligence 13, 1–13.

Cochran, S.D., Medioni, G., 1992. 3D surface description from binocular stereo. IEEE Transactions on Pattern Analysis and Machine Intelligence 14, 981–994.

Cooper, O., Campbell, N., Gibson, D., 2005. Automatic augmentation and meshing of sparse 3D scene structure. In: Proceedings 7th IEEE Workshops on Application of Computer Vision, Breckenridge, Colorado, pp. 287–293.

Forstner, W., Pertl, A., 1986. Photogrammetric standard methods and digital image matching techniques for high precision surface measurements.

In: Gelsema, E.S., Kanal, L.N. (Eds.) Pattern Recognition in Practice II. Elsevier Science Publishers B.V., New York, NY, pp. 57–72.

Fua, P., 1993. A parallel stereo algorithm that produces dense depth maps and preserves image features. Machine Vision and Applications 6, 35–49.

Fua, P., Leclerc, Y.G., 1995. Object-centered surface reconstruction: Combining multi-image stereo and shading. International Journal of Computer Vision 16, 35–56.

Hannah, M.J., 1989. A system for digital stereo image matching. Photogrammetric Engineering & Remote Sensing 55, 1765–1770.

Johanyk, Z.C., Kovacs, S., 2006. A brief survey and comparison on various interpolation based fuzzy reasoning methods. Journal of Applied Sciences at Budapest Tech Hungary 3, 91–105.

Lin, M., Tomasi, C., 2004. Surfaces with occlusions from layered Stereo. IEEE Transactions on Pattern Analysis and Machine Intelligence 26, 1073–1078.

Kanade, T., Okutomi, M., 1994. A stereo matching algorithm with an adaptive window: Theory and experiment. IEEE Transactions on Pattern Analysis and Machine Intelligence 16, 920–933.

Karner, K., 2004. MetropoGIS: A city modeling system. In: Proceedings 1st International Conference on Virtual City and Territory, Barcelona, Spain, pp. 229–234.

Kim, J., Kolmogorov, V., Zabih, R., 2003. Visual correspondence using energy minimization and mutual information. In: Proceedings 9th IEEE International Conference on Computer Vision, Nice, France, pp. 1033–1040.

Kitchen, L., Rosenfeld, A., 1982. Gray level corner detection. Pattern Recognition Letters 1, 95–102.

Kolmogorov, V., Zabih, R., Grotler, S., 2001. Computing visual correspondence with occlusions using graph cuts. In: Proceedings 7th IEEE International Conference on Computer Vision, Kerkyara, Greece, pp. 508–515.

Kolmogorov, V., Zabih, R., 2002. Multi-camera scene reconstruction via graph cuts. In: Proceedings 7th European Conference on Computer Vision, Lecture Notes in Computer Science 2352, pp. 82–96.

Larsen, M., Rudemo, M., 2004. Approximate Bayesian estimation of a 3D point pattern from multiple views. Pattern Recognition Letters 25, 1359–1368.

Matthies, L., Szeliski, R., Kanade, T., Kalman filter-based algorithms for estimating depth from image sequences. International Journal of Computer Vision 3, 209–236.

Ohta, Y., Kanade, T., 1985. Stereo by intra and inter-scanline search using dynamic programming. IEEE Transactions on Pattern Analysis and Machine Intelligence 7, 139–154.

Okutomi, M., Kanade, T., 1993. A multiple-baseline stereo. IEEE Transactions on Pattern Analysis and Machine Intelligence 15, 353–363.

Pong, T.C., Haralick, R.M., Shapiro, L.G., 1989. Matching topographic structures in stereo vision. Pattern Recognition Letters 9, 127–136.

Regattieri Delgado, M., Von Zuben, F., Gomide, F., 2000. Optimal parame-

terization of evolutionary Takagi-Sugeno fuzzy systems. In: Proceedings 8th Conference on Information Processing and Management of Uncertainty in Knowledge-Based Systems, Madrid, Spain, pp. 650–657.

Scharstein, D., Szeliski, R., 1998. Stereo matching with nonlinear diffusion. International Journal of Computer Vision 28, 155–174.

Scharstein, D., Szeliski, R., 2002. A taxonomy and evaluation of dense two-frame stereo correspondence algorithms. International Journal of Computer Vision 47, 7–42.

Scharstein, D., Szeliski, R., 2003. High-accuracy stereo depth maps using structured light. In: Proceedings IEEE Computer Society Conference on Computer Vision and Pattern Recognition, Madison, WI, pp. 195–202.

Shamir, L., 2006. Human perception-based color segmentation using fuzzy logic. In: Proceedings International Conference on Image Processing, Computer Vision and Pattern Recognition, Las Vegas, NV, pp. 496–505.

Smith, A.R., 1978. Color gamut transform pairs. Computer Graphics 12, 12–19.

Takagi, T., Sugeno, M., 1983. Derivation of fuzzy control rules from human operator's control actions. In: Proceedings IFAC Symposium on Fuzzy Information, Knowledge Representation and Decision Analysis, Marseille, France, pp. 55–60.

Takagi, T., Sugeno, M., 1985. Fuzzy identification of systems and its applications to modeling and control. IEEE Transactions on System Man & Cybernetics 20, 116–132.

Takizawa, H., Yamamoto., S., 2006. Surface reconstruction from stereo data using a three-dimensional markov random field model. IEEE Transactions on Information and Systems 89, 2028–2035.

Wood, G.A., Redlilies of automatic correlation problem. Photogrammetric Engineering & Remote Sensing 49, 537–538.

Zabin, R., Woodfill, J., 1994. Non-parametric local transforms for computing visual correspondence. In: Proceedings 3rd European Conference on Computer Vision, Stockholm, Sweden, pp. 151–158.

Zadeh, L.A., 1965. Fuzzy sets. Information and Control 8, 338–353.

Zadeh, L.A., 1974. Fuzzy Logic and its application to approximate reasoning. Information Processing 74, 591–594.

Zadeh, L.A., 1988. Fuzzy Logic. Computer 21, 83–93.

Zhou, W., Brock, R.H., Hopkins, P.F., 1996. STEREO - A digital system for surface reconstruction. Photogrammetric Engineering & Remote Sensing 62, 719–726.